35th Annual International Conference of the IEEE EMBS
Osaka, Japan, 3 - 7 July, 2013

Independent Component Analysis of EEG-fMRI data for studying epilepsy and epileptic seizures

Tiziana Franchin, Maria G. Tana, Vittorio Cannatà, Sergio Cerutti, and Anna M. Bianchi

***Abstract*—Here we present a method for classifying fMRI independent components (ICs) by using an optimized algorithm for the individuation of noisy signals from sources of interest. The method was applied to estimate brain activations from combined EEG-fMRI data for the exploration of epilepsy. Spatial ICA was performed using the above-mentioned optimized algorithm and other three popular algorithms. ICs were sorted considering the value: of the coefficients of determination R2, obtained from the multiple regression analysis with morphometric maps of cerebral matter; of the kurtosis, which features the signal energy. The validation of the method was performed comparing the brain activations obtained with those resulted using the General Linear Model (GLM). The ICA-derived activations in different datasets comprised subareas of the GLM-revealed activations, even if the volume and the shape of activated areas do not correspond exactly. The method proposed also detects additional negative regions implicated in a default mode of brain activity, and not clearly identified by GLM. Compared with a traditional GLM approach, the ICA one provides a flexible way to analyze fMRI data that reduces the assumptions placed upon the hemodynamic response of the brain and the temporal constrains.**

I. Introduction

Most existing analytical techniques for functional Magnetic Resonance Imaging (fMRI) data need specific assumptions about temporal trend of stimulation, as well as about hemodynamic profile [1]. These assumptions may be characterized by an intrinsic imprecision due the technical recordings and an inaccurate hemodynamic modeling. Data-driven analysis, such as Independent Component Analysis (ICA) [2], is a well replay for this issue, because of the possibility to characterize data without relying on the statistical testing of a few stringent hypotheses, and to generate potentially valuable information on the nature of signal and noise in the fMRI time series [3]. These are the main differences with the most commonly used "hypothesis-driven" methods, like the General Linear Model (GLM) [4], that are, instead, based on an apriori model of the impulse response of the neurovascular system.

T. F. and V. C. are with the Clinical-Technological Innovations Research Unit, Bambino Gesù Children's Hospital and Research Institute, Rome, Italy. (e-mails: tfranchin@gmail.com; vittorio.cannata@opbg.net).

M.G. T. was with the Department of Bioengineering, Politecnico of Milan, Italy. She is now with BIND – Behavioral Imaging and Neural Dynamics Center, University "G. d'Annunzio", Chieti, Italy (e-mail: mg.tana@unich.it).

S. C. and A.M. B. are with the Department of Bioengineering, Politecnico di Milano, Italy, (B. A.M., corresponding author to provide phone: +39223993342; e-mail: annamaria.bianchi@polimi.it).

Several ICA algorithms are used for biomedical applications [5], and they showed different performances according to different recorded fMRI dataset. The popular FastICA algorithm demonstrated consistent and reliable results [6], even if it loses quality performances respect to adaptive ICA algorithms when phase information has not been discarded by fMRI data recordings [7]. Moreover, comparative studies of FastICA performances showed advantages and disadvantages [8]. Zarzoso *et al.* [9] proposed an optimization method of deflection mode fixed-point algorithm (RobustICA) for improving the performance and accelerating the convergence, using kurtosis as functional in the distribution of the separator output. Both real- and complex-valued signals are treated (non-circular sources), and high convergence speed is measured in terms of source extraction quality versus number of operations.

For sorting ICs of interest from non- interest ones, various approaches were proposed as an alternative to the visual inspection: linear correlation of ICs time course with a model of the expected responses [2], which appears to contrast with the data- driven approach; a least squares Support Vector Machines (lsSVM) applied by Rodionov et al. [10] on a dataset of interictal fMRI in focal epilepsy,

Here we present a new approach for improving EEG-fMRI data analysis for epileptic patients. We optimized RobustICA algorithm using a normalized-kurtosis for taking into account the contribution of noise directly within the cost function [11]. No signal pre-processing step is required, and the effect of noise is not more considered. The results obtained by the optimized RobustICA algorithm were compared with the ones found by other three ICA algorithms (fastICA, A-CMN and ICA-EBM). For sorting the ICs identifying the significant activated areas, a new method was introduced based on the R2 statistic coefficient and the kurtosis value, which refer to the spatial and the energy contributions of the signal sources, respectively [12]. The activated regions shown by the four ICA algorithms were compared with GLM-revealed activations, for observing the possible differences in the identification of epileptic areas with or without the spatial-temporal resolution of EEG signals (essential for the GLM approach).

II. Materials and Methods

A. EEG-fMRI data

Four patients were selected by whom underwent to a Program for Surgery of Epilepsy in the Hospital of West Lisbon [13]. A first-born 2-year-old boy referred for neurophysiologic evaluation of refractoryepilepsy [14] was also added. EEG was continuously recorded with a 37-

channel system (Maglink, Neuroscan, Charlotte, NC, USA) inside a 1.5 T MR scanner (GE Cvi/NVi, Milwaukee, WI, USA). Functional MRI images were acquired with an echo-planar imaging (EPI) sequence using axial orientation (TE = 35 ms, 64 × 64 voxels, regular ascending order). For each patient, from 4 to 7 runs were acquired. Scanning parameters of fMRI acquisition are listed in Table 1. A volumetric T1 spoiled gradient recovery (SPGR) three-dimensional (3D) sequence was also acquired (0.6 mm slice thickness, in-plane resolution of 0.94 mm × 0.94 mm).

TABLE I. PARAMETERS OF FMRI ACQUISITION

Patient	*TR (s)*	*Resolution (mm × mm × mm)*	*Numbers of volumes per run*
A	2.1	4.38 × 4.38 × 5	170
B	3.12	3.75 × 3.75 × 7	100
C	2.1	4.38 × 4.38 × 5	170
D	2.33	3.75 × 3.75 × 5	150
E	2.275	3.75 × 3.75 × 5	150

B. Data preprocessing

The EEG artifacts induced during EPI acquisition were removed with the Scan 4.3.3 software (Neuroscan, Charlotte, NC, USA) and visually inspected by an experienced neurophysiologist.

The fMRI images were motion corrected, slice-timing corrected and spatially smoothed (8 mm × 8 mm × 8 mm full width at half maximum Gaussian kernel) by using SPM5 software package (http://www.fil.ion.ucl.ac.uk/).

C. Data analysis

GLM analysis of preprocessed fMRI data was performed with SPM5. The time of onset of ictal activity was convolved with canonical haemodynamic response function (HRF). HRF multivariate first order Taylor expansion in width and in time (dispersion and temporal derivative) and F-contrasts were used to perform inference on estimates of regression coefficients [13].

The same preprocessed single-subject fMRI data were analyzed using four different ICA algorithms: fastICA pow3, optimized RobustICA, A-CMN and ICA-EBM. The analysis were performed using custom-made toolboxes developed in MATLAB environment (The MathWorks Inc., Natick, MA, USA) integrated within the GIFTv1.3i software toolbox (http://mialab.mrn.org/software/gift/index.html). The significant number of independent components was selected using the Cichocki- Amari criterion [15]. Initialized parameters were set as default: all the ICA steps were run at once and back-reconstruction was performed on ICs to obtain results for individual subjects [16].

D. Description of the sorting approach

ICs were sorted using spatial regression coefficients (spatial sorting), and then measuring the kurtosis value of the ICs which are not excluded by the previous spatial sorting.

For each separated component, the R2 statistic [17] was calculated for estimating the correlation of the independent sources with the spatial template of grey and white matter of the subjects. The cerebral spinal fluid map was not considered because of the unreliability of the a-priori template [18]. This first spatial sorting is important to discard every sort of contribution it could be misleading to the realistic identification of activated areas. The criterion of selecting significant components was to choose those with a R2 value $\geq$ 0.7xR2 maximum value of all the spatial ICs [3]: threshold was imposed considering literature values [19]. Every IC which shows a R2 value less than the threshold value or presents a significant R2 value for more than one cerebral matter maps was automatically discarded by the classification.

After selection by spatial sorting, for each remaining ICs, the kurtosis values of each single was calculated. The energy contributions of the signal sources were then used to further sort and select the ICs of interest[12].

E. Evaluation of the fMRI activated regions

Spatial ICA maps were thresholded applying a Z- score statistics: a Z value of 1.5 was used in correspondence with the threshold with the threshold of $p<0.05$ for the false discovery rate control [21].

Spatial activation maps obtained by GLM and ICA analysis were compared with anatomical masks drawn by the MNI brain atlas [22], for the individuation of specific volumes of interest in each hemisphere.

III. RESULTS

A. Time performance

To quantify the computational cost, we performed 10 ICA estimations for each algorithm and for each patient (Tab. II). No comparison was implemented with GLM approach, because of the impossibility of leveling SPM procedure (above all, the statistical analysis) with ICA one.

TABLE II. TIME COMPUTATIONAL PERFORMANCE FOR EACH PATIENT USING DIFFERENT ICA ALGORITHMS

Algorithm	**Average computational time across 10 runs (s)**				
	Patient A	***Patient B***	***Patient C***	***Patient D***	***Patient E***
A-CMN	311.46	156.38	337.26	72.40	74.55
ICA-EBM	20.71	22.51	44.76	17.53	18.12
fastICA *pow3*	5.99	6.51	8.91	6.44	6.78
optimized RobustICA	5.98	6.09	10.22	5.49	5.99

B. Comparison of SPM and ICA results

For each patient and each algorithm, Table III lists the selected spatial ICs. The R2 coefficient and kurtosis values, together with the labeled activated areas are shown for each selected ICs. The outcome of the comparison between ICs and GLM maps are also listed..

TABLE III. LIST OF ICS AND ACTIVATED AREAS

Patient	*Algor.*	*R2, k*	*Regions*[a]	*GLM*[b]
A	fastICA	1.0, 18.9	FL, OTA, CER	y,y,y
		0.9, 16.6	FP	y,n
		0.7, 17.0	HG, PHPPG, FP	y,y,y
		0.7, 10.2	FP	Y

Patient	*Algor.*	*R2, k*	*Regions*[a]	*GLM*[b]
	opt. Rob.	1.0, 15.0	THA, PHPPG, FP	y,y,y
		0.9, 49.8	FP, OTA	y,y
		0.7, 12.2	FP, OL, CER	y,y,y
		0.7, 8.0	FP	y
	A-CMN	1.0, 7.7	FP	y
		0.7, 28.9	FP	y
		0.7, 6.5	CER, OTA	y,y
		0.7, 17.3	THA, PHPPG	y,y
	I-EBM	1.0, 7.7	FP	y
		0.8, 7.3	THA, PHPPG, OTA, CBL	y,y,y
		0.7, 13.2	THA, PHPPG	y
B	fastICA	1.0, 19.7	OL, OFG	y, y
		0.8, 27.3	AG, CER	y, y
		0.7, 4.1	OL, CER	y, y
	opt. Rob.	1.0, 5.7	OL	y
		0.8, 8.1	SCS, OFG, CER	y, y,y
		0.8, 5.7	OL, CER	y, y
		0.7, 7.3	AG	y
		0.7, 4.9	OL, CER	y, y
	A-CMN	1.0, 9.7	OL, SCS, OFG	y, y
		0.9, 31.3	OL, CER	y, y
		0.9,14.1	OL, AG	y, y
	I-EBM	1.0, 9.2	OL, SCS	y, y
		0.8,7.1	OFG	y
		0.3, 9.1	OL, AG, CER,	y, y,y
		0.7, 6.7	OL, CER	y, y
C	fastICA	1.0, 11.0	CER, OL, PL	y,y,y
		0.9, 15.2		
		0.8, 3.1		
	opt. Rob.	1.0, 10.0	CER, OL, PL	y,y,y
		0.9, 5.2		
		0.8, 17.1		
		1.0, 6.8		
		0.9, 8.3		
		0.8, 8.5		
	A-CMN	1.0, 5.4	CER, OL, PL	y,y,y
		0.9, 7.2		
		0.8, 5.1		
	I-EBM	1.0, 13.4	CER, OL, PL	y,y,y
		0.9, 15.2		
		0.9, 6.1		
		0.8, 9.2		
D	fastICA	1.0, 5.4	FL, PL, TL	y,y,y
		0.9, 11.5		
		0.9, 8.3		
	opt. Rob.	1.0, 15.6	FL, PL, TL	y,y,y
		0.7, 11.0		
	A-CMN	1.0, 9.8	FL, PL, TL	y,y,y
		0.9, 5.2		
		0.9, 11.1		
	I-EBM	1.0, 15.7	FL, PL, TL	y,y,y
		0.9, 7.5		
E	fastICA	1.0, 17.7	OL, CER	y,y
		0.9, 8.3	HYP, HPP	y,y
		0.8, 11.2	ACG, DLFL	y,y
	opt. Rob.	0.9, 56.1	OL	Y
		0.8, 49.2	CER	Y
		0.8, 6.2	HYP, HPP	y,y
		0.7, 29.3	ACG, DLFL	y,y
	A-CMN	1.0, 19.2	OL, CER	y, y
		0.8, 6.9	HYP, HPP	y,y
		0.7, 9.3	ACG, DLFL	y,y
	I-EBM	1.0, 20.7	HYP, HPP ACG,	y,y,y
		0.8, 4.3	DLFL, OL, CER	y,y,y

AG: angular gyrus; ACG: anterior cingulate gyrus; CBL: cerebellum; DLFL: dorso-lateral frontal lobe; FL: frontal lobe; FP: frontal pole; HEG: Heschl's gyrus; HPP: hippocampus; HYP: hypothalamus; OFG: occipital fusiform gyrus; OL: occipital lobe; OTA: occipital-temporal areas; PHPPG: parahyppocampal Gyrus; SCS: supra calcarine sulcus; TA: temporal areas; THA: thalamus; TP: temporal pole correspondence between the activated areas of interest obtained using ICA and GLM (y:yes;n: no)

Figure 1 shows clearly the differences between GLM analysis (upper row) and spatial ICs (lower row) obtained by optimized RobustICA.

For each patient, the number of voxels was estimated for each components and in the SPM maps that overlap with the corresponding masks, used for individuating the regions of interest. have very similar number of voxels coinciding with the masks. Respect to the SPM activation maps, for patient A to D, the average increase of the number of voxels estimated by ICA algorithms is of 50%, 50%, 89%, and 92% for fastICA, optimized RobustICA, A-CMN and ICA-EBM, respectively.

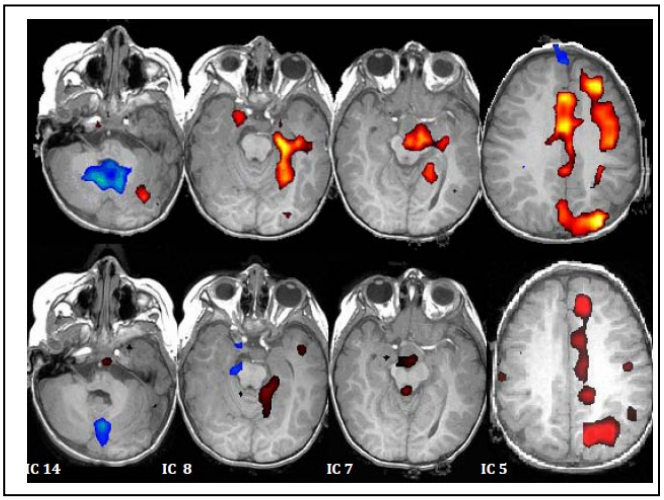

Figure 1. GLM and ICs maps of the patient E. Positive (red) and negative (blue) activations are displayed. The first row shows activated areas obtained using GLM [14]. The second raw shows activated areas of interest obtained using optimized RobustICA.

IV. Discussions

In this study we illustrated a comparisons of ICA algorithm performance in analyzing epileptic EEG-fMRI data. Four ICA algorithms were studied, showing differences in time consuming and quality performance in identifying

activated areas. The median CPU time required to run fastICA and optimized RobustICA are equal, and about a third and a twenties of the time employed by ICA-EBM and A-CMN algorithms, respectively.

An ICA approach for sorting fMRI independent components of interest was also proposed. Differently from conventional univariate statistical analyses and other ICA sorting approaches, spatial IC maps are classified by means of the only intrinsic structure of the data. The spatial contribution (R2) in ICs sorting consents to distinguish activation areas (related to vascular structure of the grey matter) from distracters ones (associated to white matter). For improving the classification, kurtosis value of IC maps is used for characterizing energetic features of the signal and then anatomical parcellation was implemented using pre-existing anatomical maps. Differently from other patients, the BOLD response associated with ictal events in gelastic epilepsy (patient E) is widespread in GLM- results respect to ICA ones, even if a considerable concurrence of activated areas exists. Increased BOLD signals were in the left HYP, HPP, OL, ACG and dorsal–lateral FL at seizure onset. Hypothalamic hamartomas (HHs) have been demonstrated as the cause of gelastic epilepsy and the neocortex becomes secondarily involved, through poorly characterized propagation pathways [15].

An important result is that ICA did not miss any GLM- revealed activation areas. Similar but still distinguishable activation patterns were obtainable with both methods. Except for the patient E, the activations appeared spatially more extended when analyzed with the ICA than with the corresponding GLM, both in group and single- case analysis. The majority of voxels missed by GLM method can be due to the specific choice of threshold suggesting that their temporal trends analyzed with GLM correlated poorly with the task timing [23]. This can explain why the inferential GLM method failed to identify specific areas. Therefore as a complementary method to GLM, ICA can be used to detect activations where the hemodynamic response differs from the model.

The last consideration about ICA is the possibility of single independent component of individuating specific activated areas, differently by GLM method in which particular software are needed to provide regions of interest (ROIs) analysis and to extract time courses from them [24].

ACKNOWLEDGMENT

The authors wish to thank Alberto Leal and the Department of Neurophysiology, Centro Hospitalar Psiquiatrico de Lisboa, for the EEG/fMRI acquisition data.

REFERENCES

[1] Y. Lu, A.P. Bagshaw, C. Grova, E. Kobayashi, F. Dubeau, J. Gotman (2006) Using voxelspecific hemodynamic response function in EEG-fMRI data analysis. *NeuroImage* 32(1): 238 – 247.

[2] M.J. McKeown, S. Makeig, G.G. Brown, T.P. Jung, S.S. Kindermann, A.J. Bell, T.J. Sejnowski. Analysis of fMRI data by blind separation into independent spatial components. *Hum Brain Mapp.* 1998;6(3):160-88.

[3] V.D. Calhoun, T.Adali, L.K. Hansen, J. Larsen, J.J. Pekar (2003) ICA of functional MRI data: an overview. In Proc. ICA-03, *International Symposium on Independent Component Analysis and Blind Signal Separation*: 281-288.

[4] KJ Worsley, KJ Friston. Analysis of fMRI time-series revisited--again. *Neuroimage*. 1995 Sep;2(3):173-81.

[5] A. Cichocki, S. Amari, *Adaptive Blind Signal and Image Processing: Learning Algorithms and Applications*, Wiley, 2003.

[6] N. Correa, T. Adali, V.D. Calhoun. Performance of blind source separation algorithms for fMRI analysis using a group ICA method. *Magn Reson Imaging.* 2007 Jun;25(5):684-94.

[7] H. Li H, N.M. Correa, P.A. Rodriguez, V.D. Calhoun, T. Adali Application of independent component analysis with adaptive density model to complex-valued fMRI data. *IEEE Trans Biomed Eng.* 2011 Oct;58(10):2794-803.

[8] Tichavsky P, Koldovsky Z, Oja E Performance analysis of the FastICA algorithm and Cramer-Rao bounds for linear independent component analysis. *IEEE Trans on Signal Process*. 2006, 54(4): 1189–1203.

[9] Zarzoso V. and Comon P., "Robust Independent Component Analysis by Iterative Maximization of the Kurtosis Contrast with Algebraic Optimal Step Size", *IEEE Transactions on Neural Networks*, Vol. 21, No. 2, February 2010, pp. 248-261.

[10] Rodionov R, De Martino F, Laufs H, Carmichael DW, Formisano E, Walker M, Duncan JS, Lemieux L. Independent component analysis of interictal fMRI in focal epilepsy: comparison with general linear model-based EEG-correlated fMRI. Neuroimage. 2007 Nov 15;38(3):488-500

[11] Wei L, Mandic DP (2006) A normalised kurtosis-based algorithm for blind source extraction from noisy measurements, Signal Process 86(7): 1580-1585.

[12] Franchin T., "Methodological Developments of the Application of Independent Component Analysis in EEGfMRI," Ph.D. dissertation, Dept. of Bioengineering., Polytechnics of Milan, Italy, 2010.

[13] Tana MG, Bianchi AM, Sclocco R, Franchin T, Cerutti S, Leal A. Parcel-based connectivity analysis of fMRI data for the study of epileptic seizure propagation. Brain Topogr. 2012 Oct;25(4):345-61.

[14] Leal AJ, Monteiro JP, Secca MF, Jordão C. Functional brain mapping of ictal activity in gelastic epilepsy associated with hypothalamic hamartoma: a case report. Epilepsia. 2009 Jun;50(6):1624-31.

[15] Cichocki A, Thawonmas R, Amari S Sequential blind signal extraction in order specified by stochastics properties, *IEE Electron. Lett*, 33 (1), 1997: 64–65.

[16] Calhoun VD, Adali T, Pearlson GD, Pekar JJ. A method for making group inferences from functional MRI data using independent component analysis. *Hum Brain Mapp.* 2001 Nov;14(3):140-51.

[17] Draper NR, Smith H *Applied Regression Analysis: Probability & Mathematical Statistics*. John Wiley & Sons, 1981.

[18] Miese FR, Wittsack HJ, Kircheis G, Holstein A, Mathys C, Mödder U, Cohnen M. Voxel-based analyses of magnetization transfer imaging of the brain in hepatic encephalopathy. World J Gastroenterol. 2009 Nov 7;15(41):5157-64.

[19] Calhoun VD, Adali T, Stevens MC, Kiehl KA, Pekar JJ (2005) Semi-blind ICA of fMRI: a method for utilizing hypothesis-derived time courses in a spatial ICA analysis, NeuroImage 25(2): 527–538.

[20] Castells F, Rieta JJ, Millet J, Zarzoso V (2005) Spatiotemporal Blind Source Separation Approach to Atrial Activity Estimation in Atrial Tachyarrhythmias, IEEE Trans Biomed Eng 52(2): 258-267.

[21] Genovese CR, Lazar NA, Nichols T (2002). Thresholding of statistical maps in functional neuroimaging using the false discovery rate. NeuroImage 15(4): 870– 878.

[22] Maldjian JA, Laurienti PJ, Kraft RA, Burdette JH. An automated method for neuroanatomic and cytoarchitectonic atlas-based interrogation of fMRI data sets. Neuroimage. 2003 Jul;19(3):1233-9.

[23] Tie Y, Whalen S, Suarez RO, Golby AJ (2008) Group independent component analysis of language fMRI from word generation tasks. NeuroImage 42(3): 1214–1225.

[24] Brett M, Anton JL., Valabregue R, Poline, JB (2002) Region of interest analysis using an SPM toolbox. NeuroImage, 16(2): 497